

THERMODESORPTION FROM CONSTRUCTION MATERIALS IRRADIATED BY IONS OF HELIUM ON A LINEAR ACCELERATOR

R.A. Anokhin, S.M. Dubniuk, B.V. Zaitsev, K.V. Pavlii, V.M. Reshetnikov, O.S. Shevchenko
National Science Center "Kharkov Institute of Physics and Technology", Kharkov, Ukraine
E-mail: sergdubnyuk@ukr.net

On a linear accelerator samples of alloys of zirconium, molybdenum and stainless steels were irradiated by beams of helium ions with an energy of 0.12...4 MeV. The results of thermal desorption of helium from irradiated samples are reported in the temperature range 20...1500°C. The results of the solution of the nonstationary equation of diffusion are presented with allowance for helium deposition profiles and damageability over the thickness of the sample. The determining factor in the formation of the second peak of thermal desorption is the shift in the maximum of the damage profile relative to the maximum profile of helium deposition in irradiated samples.

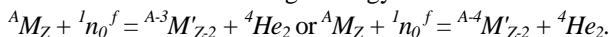
PACS: 29.27.-a

INTRODUCTION

Structural materials of nuclear power plants operate under difficult conditions of neutron irradiation, which accelerates creep processes, reduces strength and reduces deformation capacity at moderate (20...450°C), high (500...800°C) and ultrahigh (above 800°C) temperatures [1]. As a result of nuclear reactions, gaseous impurities (helium, hydrogen) are formed in the materials, promoting the appearance of helium embrittlement, hydrogen embrittlement and gas swelling. In thermonuclear reactors, the sources of helium are the products of the thermonuclear reaction (d, t), the decay of tritium, the breeding reaction:



In the volume of the material, the greatest contribution to the production of helium is due to the (*n, a*) reaction under the action of high-energy neutrons:



The source of helium in nuclear reactors are nuclear reactions in materials under the action of thermal neutrons. Comparison of helium production in fusion and fission reactors shows that the *He/dpa* ratio in nuclear reactors is about 30 to 80 times lower compared to fusion reactors [1]. The accumulation of helium in the structural materials of nuclear and thermonuclear reactors leads to a change in the physicochemical properties of the materials under irradiation [2 - 5], which indicates an increase in the negative role of helium when it is introduced into materials [6, 7]. The ratio between the rate of helium accumulation and the rate of defect formation (*He/dpa*) [8, 9], is a key parameter for many observed phenomena. The development of nuclear power generates a problem in the development of new radiation-resistant materials for new and future nuclear reactors with a view to ensuring the safety and economy of electricity produced.

The aim of the work is to irradiate the structural materials of nuclear and thermonuclear reactors on a linear accelerator of helium ions with energies of 0.12...4 MeV, followed by a study of the thermal desorption process in the temperature range 20...1500°C, as well as a mathematical description of the radiation component of the helium diffusion process taking into account the profiles of damage and deposition.

1. ACCELERATOR AND INJECTOR OF HELIUM IONS

At present, most studies of the effect of helium on the development of radiation damage have been carried out using ion implantation. To study the processes associated with implantation, a linear accelerator of helium ions with energy of up to 4 MeV operates at the NSC KIPT [10].

The accelerating section is designed to accelerate He^+ ions to 4 MeV (input energy is 30 keV/nucl.). In the accelerating structure of the counter-pin type, a method of variable-phase focusing with a step change in the synchronous phase along the focusing periods is used to focus the beam [11]. The effectiveness of this method depends on the configuration of the focusing period. The choice of synchronous phases ensured the capture of a beam of high-intensity ions in a phase angle of 120°, as well as the radial and phase stability of ion clusters along the accelerating structure. In order to ensure the maximum capture of particles (120°) in the regime of stable radial and longitudinal motion, the accelerating field in the initial part of the structure was made incremental. As a result of the calculations and experimental work performed during the setup and start-up of the accelerator section, a predetermined distribution of the electric field in the structure at the operating frequency of 47.2 MHz was obtained. The main parameters of the accelerator structure are given in Table 1.

Table 1

Options POS-4

Ion energy at the entrance, keV/nucl.	30
Energy of the accelerated ions, keV/nucl.	975
The ratio of the ion mass-to-charge	4
Operating frequency, MHz	47.2
Maximum accelerating field, kV/cm	85
Overall acceleration rate MeV/m	1.6
Resonator length, m	2.39
Cavity diameter, cm	107.5
Number of drift tubes	32
Pulse current of accelerated ions, mA	6
Input surge current, mA	30

To inject the beam into the accelerator section, an injector of singly charged helium ions was developed and fabricated. The injector consists of an ion source, a beam pulling and focusing system, and an accelerating tube. To form a beam with given parameters, a source of

the duoplasmatron type was chosen, with electrons oscillating in the anode region. The injector makes it possible to obtain a beam of singly charged helium ions with currents of several tens of milliamperes. The main parameters of the injector are given in Table 2.

Table 2

Injector parameters

The working gas	helium
Arc current, A	2...4
The beam current at the output, mA	to 20
The energy of the particles at the outlet of up to, keV	to 140
The beam diameter at the output, mm	~ 8
Working gas pressure in the anode region of the source, mm Hg	$5 \cdot 10^{-3}$
Sampling frequency, Hz	2...10
Pulse duration modulator arc, μ s	500
The magnetic field source, Oe	300...700

2. IRRADIATION, CHARACTERISTICS OF SAMPLES AND EXPERIMENTAL RESULTS

To irradiate samples from structural materials, a camera was developed and fabricated [13]. During the irradiation, the temperature of the sample, the beam current, and the irradiation dose were measured. The design of the chamber allows to change the temperature of the sample to 1000°C , allows to control the vacuum, which is carried out with the help of vacuum pumps and turbomolecular pumps up to $4 \cdot 10^{-6}$ atm. The temperature of the sample upon irradiation was measured by a chromel-alumel thermocouple attached to the sample from the opposite side with respect to the incident beam. The signal from the thermocouple was amplified by a differential amplifier. The calibration was carried out taking into account the length (~ 30 m) of the measuring wires. The current of the helium ion beam was measured by a transit sensor installed up to the sample at a distance of ~ 30 cm and graduated with the help of a Faraday cylinder installed at the exit of the accelerator, before each irradiation. The diameter of the beam of ions incident on the sample is ~ 30 mm, therefore, the area of the irradiated sample is ≈ 10 cm².

Table 3

Materials and parameters of irradiation

No	Material	Thickness of sample, μ A	Energy of ions He, MeV	Average Irradiation Temperature, $^{\circ}\text{C}$	Total radiation dose
1	Stainless steel	200	4	72	$7.5 \cdot 10^{15}$
2	Steel-3	100		78	$1.5 \cdot 10^{16}$
3	Zr+2.5% Nb	250		70	$2.3 \cdot 10^{16}$
4	Zr	300		58	$5 \cdot 10^{16}$
5	Zr+1%Nb	250	2.6	40...80	$5 \cdot 10^{16}$
6			(4+0.12)		$5 \cdot 10^{16} + 5 \cdot 10^{16}$
7			0.12		$5 \cdot 10^{16}$
8			0.12		$5 \cdot 10^{17}$
9	Nb	16	4	40	$5 \cdot 10^{16}$
10	Nb+1%Zr	22			

During the experiments on the accelerator, irradiation of samples from structural materials was carried out, the main characteristics of which are presented in Table 3.

When measuring the main radiation parameters, the analog-digital converter ZET 210 "Sigma USB" connected to a personal computer was used. This converter allows you to connect and process signal sources with different frequency ranges and perform a comparative analysis. Schemes of devices for measuring the temperature of irradiation, beam current, dose and electro-physical properties have been created.

In Fig. 1 shows the dependence of the sample temperature on the irradiation time. Similar dependences were obtained for the peak beam current and the irradiation dose versus time.

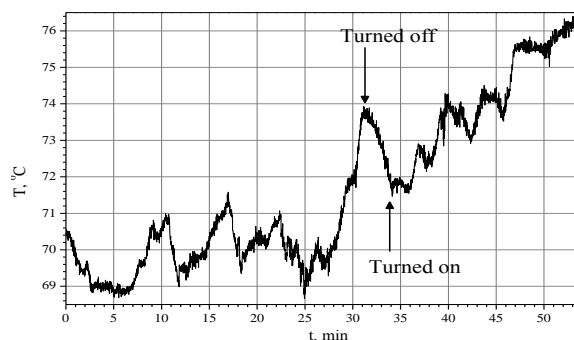


Fig. 1. Dependence of the sample temperature (stainless steel) on the time of irradiation

For all the irradiated samples, using the SRIM program, calculations were made of the distributions of damage and helium abundance in thickness. For example, in Fig. 2 shows the dependences for Zr + 1% Nb, with doses at 120 KeV and 4 MeV – identical – $5 \cdot 10^{16}$ ions. When these curves are approximated by Gaussian dependences, it follows that the dispersion decreases practically exponentially with decreasing ion energy. The damage profiles were also calculated in all irradiated samples and approximate expressions were obtained.

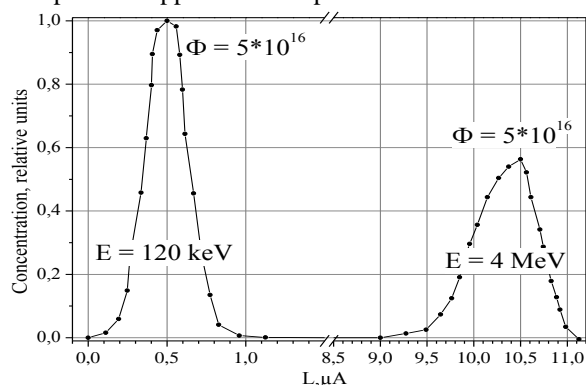


Fig. 2. The calculated profile of the distribution of helium ions implanted in Zr + 1% Nb with an energy of 120 KeV (left graph) and 4 MeV (the first graph), the dose is $5 \cdot 10^{15}$ He/cm²

The behavior of helium in the materials studied after irradiating them with helium ions with an energy of 0.12...4 MeV was studied using the thermally stimulated desorption (TD) technique. In experiments, a thermodesorption technique was used in a dynamic mode, in which the gas pressure in the chamber was proportional

to the rate of desorption from the metal. Samples were studied in the temperature range 0...1500°C. Studies of dermodiffusion were carried out [12] at the Institute of Solid State Physics, Materials Science and Technology NSC KIPT. The spectra of thermal desorption of helium from a sample of Zr+1% Nb are given in Fig. 3. More fully experimental results are presented in [13].

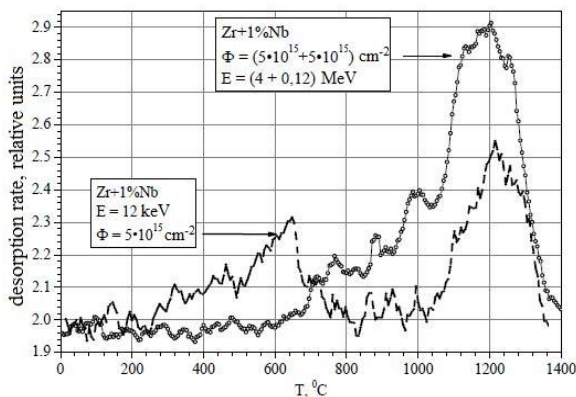


Fig. 3. Thermal desorption spectrum of helium from a sample of the Zr + 1% Nb alloy irradiated with He⁺ ions with energy 4 MeV + 120 keV (upper curve) and 120 keV (lower curve)

It can be seen from the results that appreciable gas evolution begins at $T \approx 500^\circ\text{C}$ and extends to $T \approx 1500^\circ\text{C}$. In this temperature range, the TD spectrum is characterized by a superposition of several desorption peaks. The complexity of the structure of the spectrum increases with increasing radiation dose. The maximum gassing is observed in the peak with the maximum temperature near $T \approx 1280^\circ\text{C}$. Moreover, it should be noted that this stage of desorption is observed both in the spectra of samples irradiated to a dose of $\Phi = 5 \cdot 10^{15} \text{ cm}^{-2}$ and in samples irradiated to a dose 10 times higher. A study of the gas evolution of helium from samples after their successive irradiation showed that the structure of the spectra in this case is less complicated than the spectra obtained by irradiating this alloy with 120 keV and 2.42 MeV He⁺ ions. Noticeable desorption begins at $T \approx 600^\circ\text{C}$, the peak of gas evolution with a maximum at $T \approx 1200^\circ\text{C}$ predominates in the spectrum.

3. DESCRIPTION OF HELIUM DIFFUSION FROM IRRADIATED SAMPLES

From an analysis of the experimental data, it follows that the presence of several peaks in the TD spectra indicates the existence of several discrete stages of helium separation, distinguished by the mechanisms of helium escape from the metal. Upon irradiation, helium atoms interact with crystal lattice defects, which are traps for helium. In this case, helium is captured by single vacancies, divacancies, clusters of vacancies. And also helium is captured by dislocations and grain boundaries, interphase boundaries, formation of helium and helium-vacancy clusters [1]. Traps for their ability to absorb and release diffusion-bearing atoms are conventionally divided into three groups: with negligible retention capacity; traps, which are constant for all temperatures and times of the experiment, capable of absorbing and releasing diffusing atoms; traps which, at the temperature of the experiment, firmly hold the diffusing atoms.

In addition, the effective diffusion coefficient has a temperature dependence including the activation energy, which is the sum of the activation energies for simple interstitial diffusion and the contribution from the binding energy in the trap. On the diffusing substance, in our case – helium, the external force acts in the process of diffusion. Then, a flux caused by the action of an external force field will be superimposed on the flow of matter JD, $J_v = C\bar{v}$ (\bar{v} – the directed velocity of the substance acquired under the influence of the field), and the total flux of the diffusant can be written as follows:

$$J = -D(\partial C/\partial x) + C\bar{v}.$$

In our case, it is necessary to determine the role of the radiation component, expressed as a function of damage from the thickness of the sample, and the profile of helium deposition implanted in the sample. In describing diffusion processes, the role of defects in materials can be taken into account in two ways: by modifying differential equations or by modifying the diffusion coefficient itself, leaving the differential equation in its original form. You can also use a combination of these approaches. To describe the diffusion of helium from irradiated structural materials, we used the equation in the form:

$$\frac{\partial C}{\partial t} = D_{\text{eff}} \cdot \frac{\partial^2 C}{\partial x^2} + \bar{v} \cdot \frac{\partial C}{\partial x}, \quad (1)$$

with the following boundary conditions:

$$\frac{\partial C(0, t)}{\partial x} = 0, \quad \frac{\partial C(h_{\text{max}}, t)}{\partial x} = 0, \quad (2)$$

where h_{max} is the maximum range of helium ions in the sample under irradiation; C – is the concentration, t – is the time; x – is the coordinate (the diffusion thickness of the sample); \bar{v} – is the diffusion rate determined by the following expression:

$$\bar{v} = -D_{\text{eff}} \frac{\partial}{\partial x} \ln C, \quad (3)$$

where D_{eff} – is the effective diffusion coefficient, which was determined from the experimental data. In Fig. 4 shows the dependence of the effective diffusion coefficient of helium on the temperature for Zr+1% Nb. It follows from the dependence that a phase transition of the irradiated material Zr+1% Nb is observed in the temperature range 660...800°C. The same conclusion follows from Fig. 5.

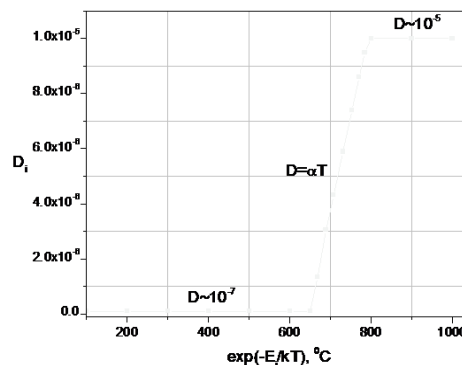


Fig. 4. Dependence of the diffusion coefficient on the temperature for Zr + 1% Nb

This is the experimental temperature dependence of the heated sample from the time, obtained with a linear change in the heating power. From Fig. 5 that the slope of the curve decreases in the range of 660...800°C, which also confirms the presence of a phase transition.

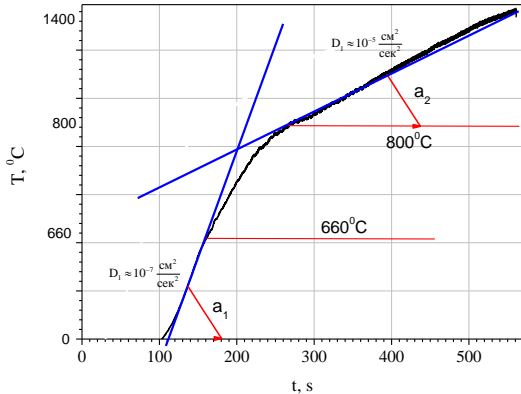


Fig. 5. Experimental dependence of the sample heating temperature on time (sample – Zr + 1% Nb)

These changes must be taken into account in equation (1) in determining the effective diffusion coefficient in the following form:

$$D_{\text{eff}} = D_0 \begin{cases} \text{Const}_1, & T < 660^\circ\text{C}, \\ \alpha T, & 660^\circ\text{C} < T < 800^\circ\text{C}, \\ \text{Const}_2, & T > 800^\circ\text{C}, \end{cases} \quad (4)$$

where α – is the proportionality coefficient. In the first approximation, linear dependence can be used. This dependence should be taken into account only in the presence of phase transitions.

The initial conditions for equation (1) were obtained by approximating the profile of the distribution of helium for Zr+1% Nb and have the form:

$$C(x, t = 0) = C_m \begin{cases} 2907.17 \exp\left(-6.67(x - 10.68)^2\right) & x < 10.68 \\ 2907.17 \exp\left(-24.58(x - 10.68)^2\right) & x > 10.68, \end{cases}$$

where C_m was normalized to the total radiation dose:

$$\Phi t = \int_0^{h_{\text{max}}} C(x, t = 0) \cdot dx \Rightarrow C_m.$$

The account of the damageability of the sample, after its irradiation on the accelerator, was taken into account in the diffusion coefficient as follows. The diffusion coefficient can be represented:

$$D_0 = D_i \frac{\overline{\text{DPA}}}{\text{DPA}(x)},$$

where $\overline{\text{DPA}}$ – the average number of displacements at the diffusion length, $\text{DPA}(x)$ – the function of the distribution of the damage profile, which for Zr+1% Nb is written:

$$\text{DPA}(x) = \text{DPA}_m \begin{cases} \frac{0.012}{(x - 10.56)^2 + 0.1028}, & x < 10.56 \\ 0.1941 \exp\left(-13.16(x - 10.56)^2\right), & x > 10.56. \end{cases}$$

The average number of offsets is determined by:

$$\overline{\text{DPA}} = \frac{1}{h_{\text{max}}} \int_0^{h_{\text{max}}} \text{DPA}(x) \cdot dx$$

and is normalized to the radiation dose, taking into account the energy required for a single bias (K – the number of displacements per ion):

$$K \cdot \Phi t = \int_0^{h_{\text{max}}} \text{DPA}(x) \cdot dx \Rightarrow \text{DPA}_m.$$

Then the effective diffusion coefficient can be represented in the form:

$$D_{\text{eff}} = D_0 \exp\left\{-\frac{E_i}{kT(t)}\right\},$$

where E_i – is the activation energy; T – is the temperature that is changed during the experiment; k – is the Boltzmann constant. Numerically solving the diffusion equation, taking into account the distribution functions of helium and damage and taking into account the experimental parameters, namely, the temperature change from time to time, the calculated thermodesorption curves of helium from irradiated samples were obtained. In Fig. 6 shows the calculated and experimental dependences of helium desorption from a Zr+1% Nb sample irradiated by helium ions with an energy of 4 MeV on a linear accelerator.

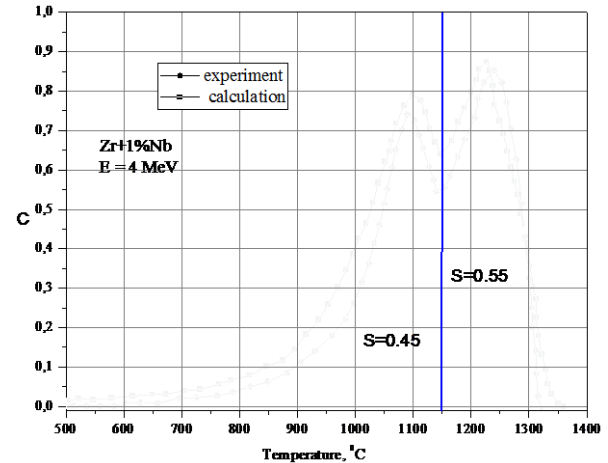


Fig. 6. Calculated (upper curve) and experimental (lower curve) desorption curves from a Zr + 1% Nb sample irradiated with helium ions with an energy of 4 MeV

It follows from the calculations that the maximum of the damage profile is shifted to the surface of the sample on which the beam was incident, in relation to the maximum profile of helium deposition. In this case, the problem can be interpreted as the motion of helium in the field of radiation damage. This effect explains the appearance of a second peak on the desorption curve.

CONCLUSIONS

On a linear accelerator of helium ions with energies 0.12...4 MeV, irradiation of structural materials was carried out with subsequent study of thermal desorption. In the description it was shown that the second peak on the desorption graph is formed due to the shift of the maximum of the radiation damage relative to the maximum of helium deposition.

REFERENCES

1. I.M. Neklyudov, G.D. Tolstolutskaia. Helium and hydrogen in structural materials // *Problems of Atomic Science and Technology. Series "Physics of Radiation Effects and Radiation Materials Science"*. 2003, № 3, p. 3-14.
2. H. Ullmaier. The influence of helium on the bulk properties of fusion reactor structural materials // *Nuclear fusion*. 1984, v. 24, № 8, p. 1039-1083.
3. V.F. Zelensky, I.M. Neklyudov, T.P. Chernyaeva. *Radiation defects and swelling of metals*. Kiev: "Naukova Dumka", 1988, 296 p.
4. A.I. Ranyuk, V.F. Rybalko. *Helium in a lattice of metals: Review*. M.: "CRIAtominform", 1986, p. 64.
5. I.M. Neklyudov, V.F. Rybalko, G.D. Tolstolutskaia. *Evolution profiles of helium and hydrogen in materials during irradiation and annealing*. M.: "CRIAtominform", 1985, p. 41.
6. I. Mukouda, Y. Shimomura, T. Iiyama, et al. Microstructure in pure copper irradiated by simultaneous multiion beam of hydrogen, helium and self ions // *J. of Nucl. Mater.* 2000, v. 283-287, p. 302-305.
7. B.H. Sencer, G.M. Bond, F.A. Garner, et al. Microstructural evolution of alloy 718 at high helium and hydrogen generation rates during irradiation with 600...800 MeV protons // *J. of Nucl. Mater.* 2000, v. 283-287, p. 324-328.
8. E.E. Bloom. Mechanical properties of materials in fusion reactor first-wall and blanket systems // *J. of Nucl. Mater.* 1979, v. 85 and 86, p. 795-799.
9. V.O. Bomko, A.M. Yegorov, B.V. Zaytsev, A.F. Kobets, K.V. Pavlii. Development of the "MILAC" complex for nuclear physical investigation // *Problems of Atomic Science and Technology. Series "Nuclear Physics Investigations"*. 2008, №3(49), p. 100-104.
10. V.A. Bomko, A.P. Kobets, S.S. Tishkin, et al. Variant of alternating phase focusing with the stepped change of the synchronous phase // *Problems of Atomic Science and Technology. Series "Nuclear physics investigations"*. 2004, № 2, p. 153-155.
11. I.M. Neklyudov, V.N. Voyevodin, V.V. Ruzhitsky, et al. A combination of the method of nuclear reactions, thermal de-sorption spectrometry, and two-beam irradiation in studying the behavior of helium and hydrogen in structural materials // *Proceedings of the XIV International Meeting "Radiation Physics of Solids"*, Sevastopol, July 5-10, 2004, p. 592-596.
12. R.A. Anokhin, V.N. Voyevodin, S.N. Dubnyuk, et al. Methods and experimental results constructions materials irradiation of helium ions at the linear accelerator // *Problems of Atomic Science and Technology. Series "Physics of Radiation Effects and Radiation Materials Science"*. 2012, №5(81), p. 123-130.

Article received 09.10.2017

ТЕРМОДЕСОРБЦИЯ ИЗ КОНСТРУКЦИОННЫХ МАТЕРИАЛОВ, ОБЛУЧЕННЫХ ИОНАМИ ГЕЛИЯ НА ЛИНЕЙНОМ УСКОРИТЕЛЕ

Р.А. Анохин, С.Н. Дубнюк, Б.В. Зайцев, К.В. Павлий, В.Н. Решетников, А.С. Шевченко

На линейном ускорителе были облучены образцы сплавов циркония, молибдена и нержавеющей сталей пучками ионов гелия с энергией 0,12...4 МэВ. Приведены результаты термодесорбции гелия из облученных образцов в диапазоне температур 20...1500°C. Представлены результаты решения нестационарного уравнения диффузии с учетом профилей залегания гелия и повреждаемости по толщине образца. Определяющим фактором образования второго пика термодесорбции является сдвиг максимума профиля повреждаемости относительно максимума профиля залегания гелия в облученных образцах.

ТЕРМОДЕСОРБЦІЯ З КОНСТРУКЦІЙНИХ МАТЕРІАЛІВ, ОПРОМІНЕНИХ ІОНАМИ ГЕЛІЮ НА ЛІНІЙНОМУ ПРИСКОРІЮВАЧІ

Р.А. Анохін, С.М. Дубнюк, Б.В. Зайцев, К.В. Павлій, В.М. Решетніков, О.С. Шевченко

На лінійному прискорювачі були опромінені зразки сплавів цирконію, молибдену і нержавіючих сталей пучками іонів гелію з енергією 0,12...4 МеВ. Наведено результати термодесорбції гелію з опромінених зразків у діапазоні температур 20...1500°C. Представлені результати рішення нестационарного рівняння дифузії з урахуванням профілів залягання гелію і пошкоджуваності по товщині зразка. Визначальним фактором виникнення другого піку термодесорбції є зрушення максимуму профілю пошкоджуваності щодо максимуму профілю залягання гелію в опромінених зразках.